Sci. Bull. (2015) 60(21):1807–1823
DOI 10.1007/s11434-015-0914-9

www.scibull.com
www.springer.com/scp

Review

Engineering Sciences

Recent advances in nanoporous graphene membrane for gas separation and water purification

Chengzhen Sun · Boyao Wen · Bofeng Bai

Received: 19 August 2015 / Accepted: 22 September 2015 / Published online: 14 October 2015

Abstract Graphene is a one-atom-thick sheet of graphite comprising sp^2-hybridized carbon atoms arranged in the hexagonal honeycomb lattices. By removing the honeycomb lattices and forming nanopores with specific geometry and size, nanoporous graphene has been demonstrated as a very high-efficiency separation membrane, due to the ultrafast molecular permeation rate for its one-atom thickness. This review focuses on the recent advances in nanoporous graphene membrane for the applications of gas separation and water purification, with a major emphasis on the molecular permeation mechanisms and the advanced fabrication methods of this state-of-the-art membrane. We highlight the advanced theoretical and experimental works and discuss the gas/water molecular transport mechanisms through the graphene nanopores accompanied with theoretical models. In addition, we summarize some representative membrane fabrication methods, covering the graphene transfer to porous substrates and the pore generation. We anticipate that this review can provide a platform for understanding the current challenges to make the conceptual membrane a reality and attracting more and more attentions from scientists and engineers.

Keywords Nanoporous graphene · Gas separation · Water purification · Molecular permeation mechanism · Membrane fabrication

C. Sun · B. Wen · B. Bai (✉)
State Key Laboratory of Multiphase Flow in Power Engineering, Xi'an Jiaotong University, Xi'an 710049, China
e-mail: bfbai@mail.xjtu.edu.cn

1 Introduction

Graphene [1–3] is a two-dimensional one-atom-thick sheet of sp^2-bonded carbon atoms packed in the honeycomb crystal lattices, exhibiting good chemical stability [4, 5], excellent thermal conductance [6–8], strong mechanical strength [9, 10], and remarkable electronic properties [11–13]. The unique property of graphene, i.e, one-atom thickness, results in many promising applications in a wide range of fields [14], especially in separation science. It is demonstrated that the pristine graphene is permeable to proton [15, 16], but impermeable to any molecules, even the smallest helium atoms [17–19]. However, the graphene sheet featuring nanopores formed by selectively removing carbon atoms, called as nanoporous graphene (NPG) [20, 21], has been proposed as a very promising size-selective separation membrane based on the molecular sieving effects. As said by the editors of *Nature Nanotechnology* [22], "Graphene opens up to new applications—Effective separation membranes could be created by etching nanometer-sized pores in two-dimensional materials". Owing to the one-atom thickness of graphene itself, the transport rates of molecules through the NPG membranes are expected to be extremely high. Several studies [23–26] numerically and experimentally suggested that the NPG membranes can exhibit high permeability and selectivity exceeding those of existing state-of-the-art polymer membranes by orders of magnitude. Meanwhile, high-quality graphene fabrication [27–30], transfer to porous substrates [31–33], and pore generation [25, 34–39] methods are being developed very well, making the NPG separation membranes very promising in the near future. Recently, another graphene-related material—graphene oxide—was also demonstrated as an efficient separation membrane [40–51]. Graphene oxide is an analogue of graphene by

asymmetrically modified with oxygen-containing functional groups (hydroxyl, epoxy groups, carboxyl, carbonyl, phenol etc.) on the edges and planes. The separation of hybrid molecules using graphene oxide membranes is realized by the selective molecular diffusion in the interlayer spacing between the oxygen-containing groups on the graphene sheets, the structural defects within graphene oxide flakes, etc. The advantages of graphene oxide membranes include ease of synthesis, ease of scale-up and easy of reassembled into large-area film, but at the cost of permeance that is much smaller than those predicted for the single-layer NPG membranes. Therefore, NPG membrane is the limit of membranes, and its permeance can achieve the theoretical maximum, deserving the attentions from scientists and engineers.

In 2009, Jiang et al. [24] firstly proposed that the NPG with specific pore size and geometry would be a very efficient gas separation membrane using first principle calculations (Fig. 1a). They found a high selectivity on the order of 10^8 through an N-functionalized pore and an extremely high selectivity on the order of 10^{23} through an all-H passivated pore for separating H_2/CH_4 mixtures with a high H_2 permeance. Afterward, several theoretical works were conducted to further confirm that the NPG membranes could achieve high permeability and selectivity for gas separations [23, 52–55]. Due to the difficulties in experimental works,

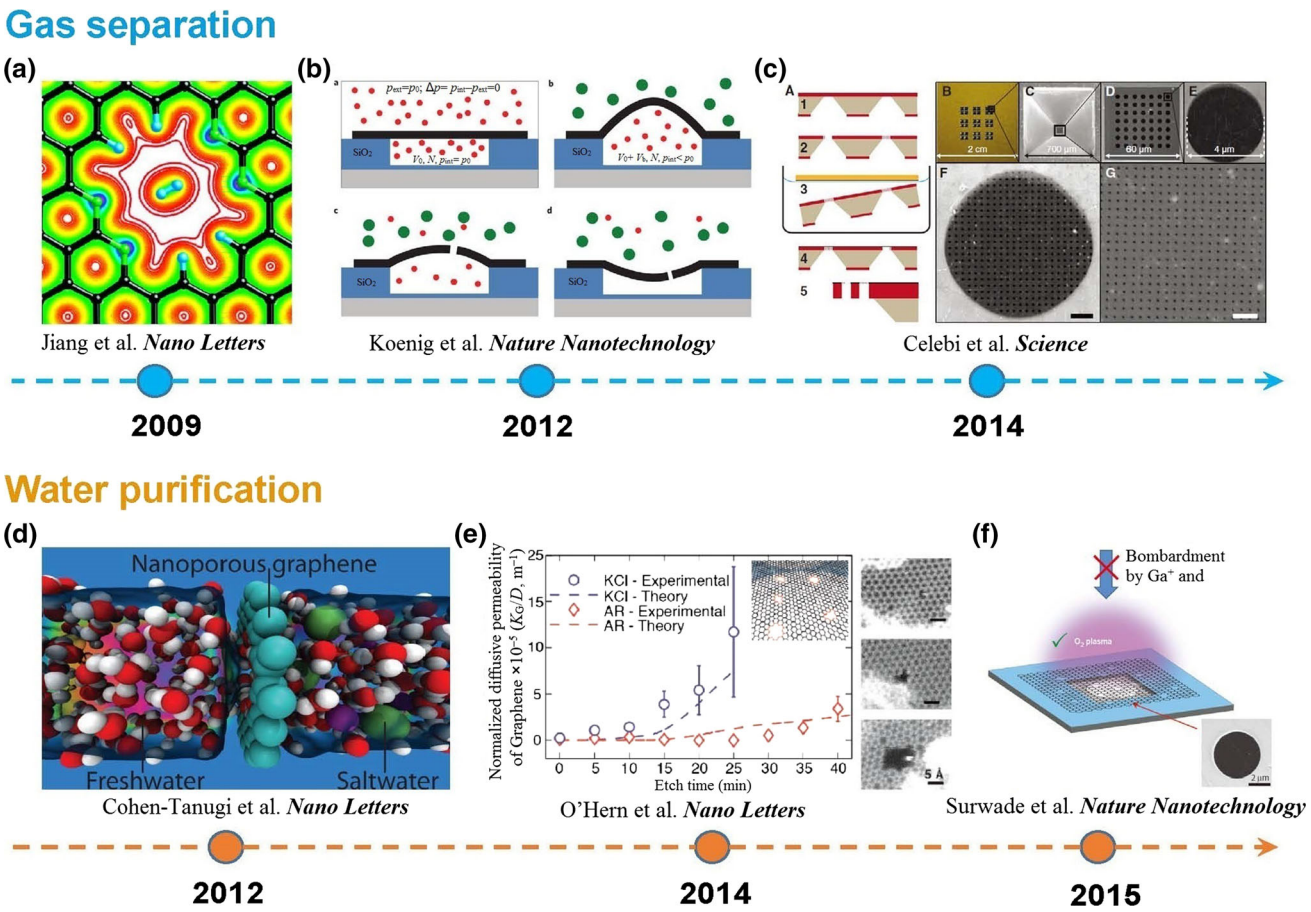

Fig. 1 (Color online) Development history for NPG membranes in the applications of gas separation and water purification. **a** Electron density isosurface of the all-H pore edge passivated NPG. Reprinted with permission from Ref. [24], Copyright 2009, American Chemical Society. **b** Measurement system of the gas transport through micrometer-sized NPG membranes. Reprinted with permission from Ref. [25], Copyright 2012, Nature Publishing Group. **c** Fabrication procedure of the NPG membrane for gas separation. Reprinted with permission from Ref. [56], Copyright 2014, American Association for the Advancement of Science. **d** Atomic view of water desalination by a NPG membrane. Reprinted with permission from Ref. [57], Copyright 2012, American Chemical Society. **e** Permeability of different molecules versus the pore etching time. Reprinted with permission from Ref. [58], Copyright 2014, American Chemical Society. **f** Schematic of single-layer graphene suspended on a 5-μm-diameter hole. Reprinted with permission from Ref. [59], Copyright 2015, Nature Publishing Group

the first measurement on the gas transport through NPGs was launched in 2012 by Koenig et al. [25] (Fig. 1b). They used a pressurized blister test and mechanical resonance to measure the transport rates of a variety of gases (H_2, CO_2, Ar, N_2, CH_4, and SF_6) through the graphene nanopores, created by ultraviolet-induced oxidative etching. However, their measurement just involved the micrometer-sized graphene membrane, which was far away from the industrial scale. In 2014, Celebi et al. [56] reported a high transport rate for numerous gases across physically perforated double-layer graphene featuring pores with narrowly distributed diameters (Fig. 1c). The area of the membrane they fabricated reached up to square millimeters. Their work demonstrated that the industrial-scale NPG-based gas separation membrane is possible in the current technical world.

For water purification, it was firstly proposed by Cohen-Tanugi and Grossman [57] in 2012 (Fig. 1d). They reported that the nanometer-scale pores in a single-layer freestanding graphene can effectively filter NaCl salt from water using classical molecular dynamics (MD) simulations. Their results indicated that the water permeability of the NPG membranes was several orders of magnitude higher than those of the conventional reverse osmosis membranes. An experimental work was conducted soon by O'Hern et al. [58] in 2014, in which the transport rates of various ions through the high-density sub-nanometer pores (diameters 0.40 ± 0.24 nm and densities exceeding 10^{12} cm^{-2}) in the macroscopic single-layer NPG membranes were measured (Fig. 1e). Subsequently, in 2015 Surwade et al. [59] showed that the single-layer NPGs, with oxygen plasma-etched nanometer-sized pores, can be used as a desalination membrane. The NPG membrane they fabricated exhibited a salt rejection rate of nearly 100 % and a water transport flux up to 10^6 g m^{-2} s^{-1} at 40 °C using pressure difference as a driving force (Fig. 1f).

In summary, the NPG membrane has shown promise for applications in gas separation, water purification and other fields, such as hydrogen generation and storage [15, 16, 53, 60], isotope separation [61–64], molecular valve [65], and DNA sequencing [66–68]. Here, we review the recent advances in the development of NPG membranes for gas separation and water purification, including the theoretical and experimental studies. Particularly, we put emphasis on discussing the gas/water molecular transport mechanisms through the NPG membranes and the advanced fabrication methods of this state-of-the-art membrane. We anticipate that this review can help the scientists and engineers understand the current challenges to make the conceptual efficient membrane a reality and develop it in the industrial applications.

2 Gas separation

2.1 Theoretical work

We firstly highlight the recent advanced theoretical works on the NPG gas separation membranes. After putting forward the conception of NPG gas separation membrane, many theoretical works were conducted, mainly using MD simulation method and density functional theory. Most of these works focused on how fast the gas transport through the NPG membranes and how high the selectivity for separating mixture gases. The permeation processes of many kinds of gas molecules through the NPG membranes with various pore sizes and geometries were involved in the theoretical works. In the aspect of MD simulation works, Schrier [69] reported a CO_2 permeance of 4×10^5 GPU (gas permeation unit, 1 GPU $= 3.35 \times 10^{-10}$ mol s^{-1} m^{-2} Pa^{-1}) through a special porous graphene extended in one direction by an E-stilbene-like unit. Tao et al. [70] also found that this special NPG membrane exhibited a high permeance of H_2, CO, N_2, and CH_4 molecules. Wu et al. [71] observed a higher selectivity of the F-modified porous graphene for separating CO_2/N_2 mixtures (the atomic view of this separation process can be found in Fig. 2a). Liu et al. [72, 73] reported a permeance of H_2 in the range of 1×10^5–4×10^5 GPU and a permeance of CO_2 on the order of 10^5 GPU through a 10-unit pore modified by 4 N atoms and 4 H atoms. They also gave a flux sequence of different molecules, i.e., $H_2 > CO_2 \gg N_2 > Ar > CH_4$, through this special pore, which generally followed the trend of the molecular kinetic diameters [74]. Sun et al. [75] identified high permeability (10^5–10^6 GPU) and selectivity (10^2) for separating the CH_4/CO_2, CH_4/H_2S and CH_4/N_2 mixtures using the N- and H-functionalized graphene nanopores. Lu et al. [76] found a high selectivity for H_2 relative to CO, CH_4, and CO_2 through the graphene nanopores doped by B and N atoms. Nieszporek and Drach [77] noted a high selectivity for the CH_4/C_4H_{10} mixture through the H-passivated pore of diameter 0.32 nm. Du et al. [23] designed a series of NPGs as the membranes for separating the H_2/N_2 mixtures and observed more permeation events of N_2 than those of H_2 molecules for the big nanopores, while Sun et al. [78] found that the permeation flux of different molecules increased with the increase of pore size in the same trend and the flux of big molecules even exceeded that of small molecules, such as $H_2 >$ He and $CH_4 > N_2$. In the MD simulations, the permeance (P) of gas molecules can be obtained via the relationship between the molecular crossing number (N) through graphene nanopores and the time (t). In the equilibrium and non-equilibrium systems, the function $N = f(t)$ is different, and thus the way to

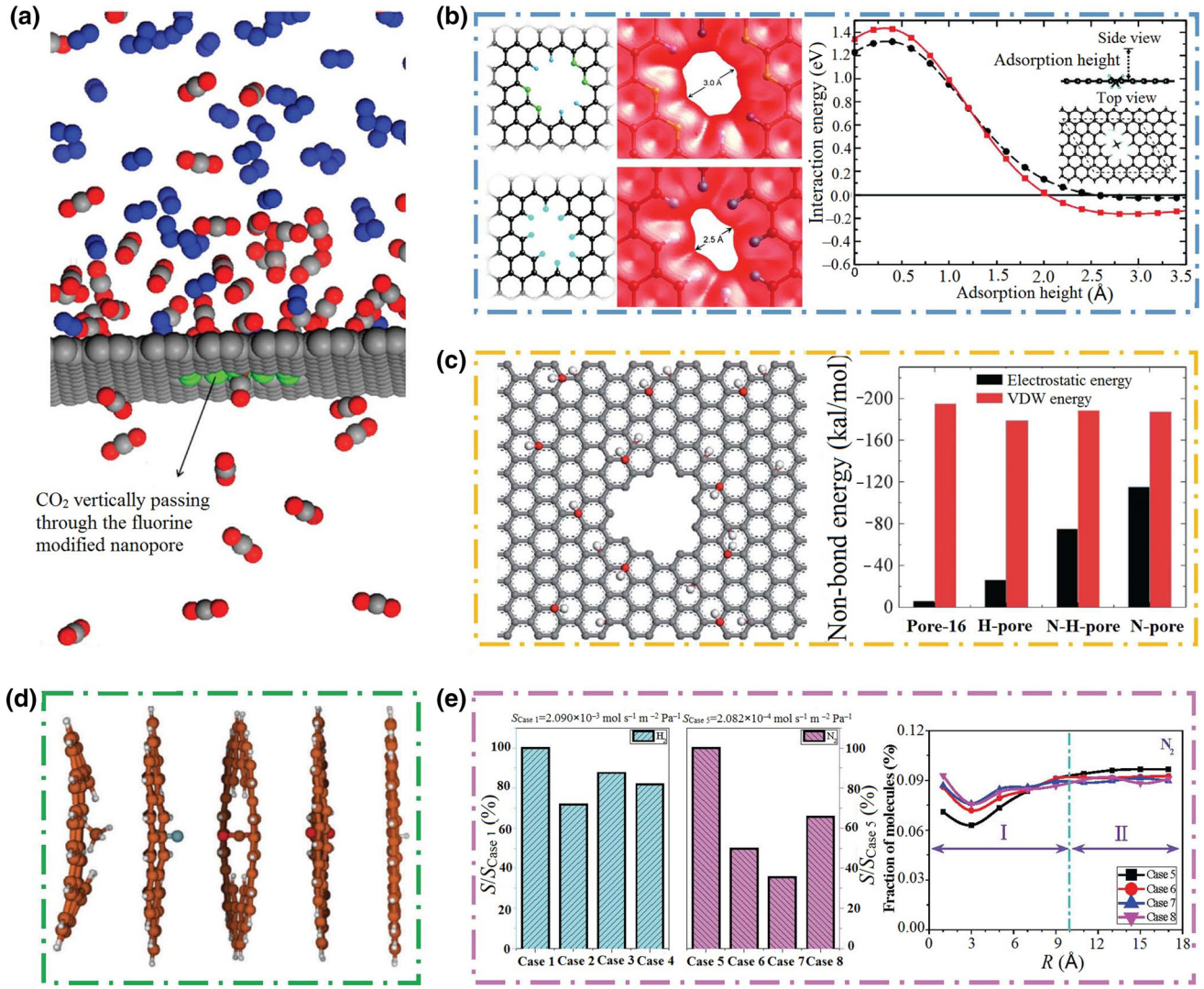

Fig. 2 (Color online) Theoretical works on NPG membranes for gas separation. **a** Atomic system configuration for the separation of CO_2/N_2 mixtures. Reprinted with permission from Ref. [71], Copyright 2014, American Chemical Society. **b** Interaction energy between CH_4 and the all-H-passivated porous graphene as a function of adsorption height. Reprinted with permission from Ref. [24], Copyright 2009, American Chemical Society. **c** Van der Waals energy and electrostatic energy of the system with a surface functionalized NPG membrane. Reprinted with permission from Ref. [83], Copyright 2012, Royal Society of Chemistry. **d** Geometry distortions of pores caused by the propagation of the gas molecules. Reprinted with permission from Ref. [80], Copyright 2012, Royal Society of Chemistry. **e** Inhibition and blocking effect of non-permeating components on the permeation of permeating component. Reprinted with permission from Ref. [86], Copyright 2015, Royal Society of Chemistry

obtain the permeance is totally different. The selectivity of species A relative to species B ($S_{A/B}$) is equal to the ratio of P_A and P_B ($S_{A/B} = P_A/P_B$). Usually, researchers often adopt a parameter $F_{A/B}$ to reflect the selectivity, although $F_{A/B} \neq S_{A/B}$. The parameter $F_{A/B}$ is defined as

$$F_{A/B} = \frac{y_A/y_B}{x_A/x_B}, \quad (1)$$

where x_A is the mole fraction of species A in the feed side, y_A is the mole fraction of species A in the permeate side, x_B is the mole fraction of species B in the feed side, and y_B is the mole fraction of species B in the permeate side.

For the density functional theoretical works, Jiang et al. [24] found the high selectivities and H_2 permeance for separating H_2/CH_4 by the NPGs with N-functionalized and all-H-passivated pores (Fig. 2b). Schrier [54] demonstrated that the NPGs can separate He from other noble gases and alkanes (e.g., Ne, CH_4), and the quantum mechanical effects played a quantifiable role in the permeability. Ambrosetti and Silvestrelli [79] evaluated the permeation barriers of the H_2O,

CH_4, CO, CO_2, O_2, H_2 molecules and Ar atom through the H-saturated pores and observed that the nontrivial H-bond interactions with the pore-saturating H atoms caused a low permeation barrier of H_2O molecules. Hauser and Schwerdtfeger [80] compared the reaction barrier energies of CH_4, N_2, O_2, CO_2, and H_2 molecules and showed that the two-ring pores were effective for the separation of CH_4 from other gases. Blankenburg et al. [52] displayed an extremely high selectivity of a specific nanopore for H_2 and He relative to other atmospheric gases, e.g., Ne, O_2, N_2, CO, CO_2, NH_3, and Ar. Tao et al. [70] and Wu et al. [71] also demonstrated that the NPG membranes can achieve excellent performance for the CO_2/N_2 separation and hydrogen purification. Qin et al. [81] showed a strong barrier of 1.5 eV for CH_4 but an weak barrier of only 0.12 eV for H_2 to separate the CH_4/H_2 mixtures using the NPGs consisting of octagons and all-H-passivated pores. In the density functional theory calculations, the lower the diffusion barriers, the faster the molecules transport through the NPG membranes. The selectivity is usually obtained based on the diffusion barriers of different molecules using the Arrhenius equation,

$$S_{A/B} = \frac{D_A}{D_B} = \frac{C_A}{C_B} \frac{e^{-E_A/RT}}{e^{-E_B/RT}}, \quad (2)$$

where D is the diffusion rate, C is the prefactor, E is the diffusion barrier, R is the universal gas constant, T is the temperature, and A and B are two kinds of gas species.

The permeation of gas molecules through NPG membranes is affected by many factors, including the adsorption of molecules on the graphene surface [23, 82], the chemical functionalization of pore rim and surface [71, 83], the geometry distortion of the NPG membrane [80], and the charges on the pore [84]. These influencing factors were mainly identified in the theoretical works. Du et al. [23] and Sun et al. [78] both demonstrated that the adsorption of gas molecules on the graphene surface was beneficial for the molecular permeation through the NPGs. Shan et al. [83] revealed that the adsorption ability of CO_2 molecules on the graphene surface increased after a chemical functionalization of the graphene sheet, and the selectivity of CO_2 over N_2 significantly improved with the chemical functionalization of the pore edge (Fig. 2c). Wu et al. [71] found that after the F-modification on the pore rim, the diffusion barrier of CO_2 decreased while that of N_2 greatly increased, thus improving the selectivity for the CO_2/N_2 separation. Lu et al. [76] achieved a significant improvement in the hydrogen purification from mixture gases through the doping of B or N atoms on graphene nanopores. Hauser and Schwerdtfeger [80] found that the pore structure relaxation effects can reduce the diffusion barriers significantly. They suggested that this effect need to be taken into account for the better predictions of gas permeabilities (Fig. 2d). Lei et al. [84] evaluated the effect of pore charges on the separation of H_2S/CH_4 mixtures and observed more H_2S molecules around the charged pore. The selectivity was improved due to the electrostatic interactions between H_2S molecules and graphene atoms. Huang et al. [85] demonstrated that the permeance (2.4×10^5 GPU for H_2) and selectivity (10^{24} at room temperature) were significantly improved for the separation of H_2/CH_4 by adopting an inter-layer-connected porous graphene bilayer. In a recent work by Wen et al. [86], an inhibition effect of non-permeating components on the permeation of permeating component was identified (Fig. 2e). They attributed this phenomenon to two reasons: one was the relatively weakening contribution of surface adsorption on the molecular permeation, and another was the blocking effect of non-permeating molecules around the nanopore (Fig. 2e). Many other influencing factors are expected to be examined by conducting theoretical works, because they are more practicable than experimental works. Meanwhile, the models in the theoretical works should be more close to the real systems in the experiments, such as pore size, porosity, pore structure, and membrane constitution.

2.2 Experimental work

Comparing to the theoretical works, the experimental works on the NPG gas separation membrane are very limited due to the difficulties for conducting such nanoscale measurements. The experimental works mainly focused on the fabrication of NPG membranes and the measurements of gas transport rates. The first experimental measurement was performed by Koenig et al. [25]. They produced the nanopores in a micrometer-sized graphene membrane using ultraviolet-induced oxidative etching and measured the transport rates of H_2, CO_2, Ar, N_2, CH_4, and SF_6 gases. Their results showed that in some cases the permeation flux of big molecules (CH_4) exceeded that of small molecules (N_2), and the measured data were consistent with the theoretical values in the literature (Fig. 3a). Intrinsic defects inevitably exist, and thus the gas transport through defects is unavoidable and can critically affect the separation performance. Understanding of the role of defects in mass transport across single-layer and multi-layer NPG membranes is of crucial importance. Boutilier et al. [87] reported a systematic experimental and theoretical investigation of the gas transport through the graphene membranes with intrinsic defects. It was revealed that the selective transport could be achieved in the presence of non-selective defects. They demonstrated an exponential reduction in the gas flow rates with independent stacking of the graphene layers and developed a model of gas transport to explain this behavior as the random probability of defect overlap (Fig. 3b). They also showed that the size and permeance of the pores in the porous support substrate critically affected the separation performance and revealed the parameter spaces where effective gas separation can be

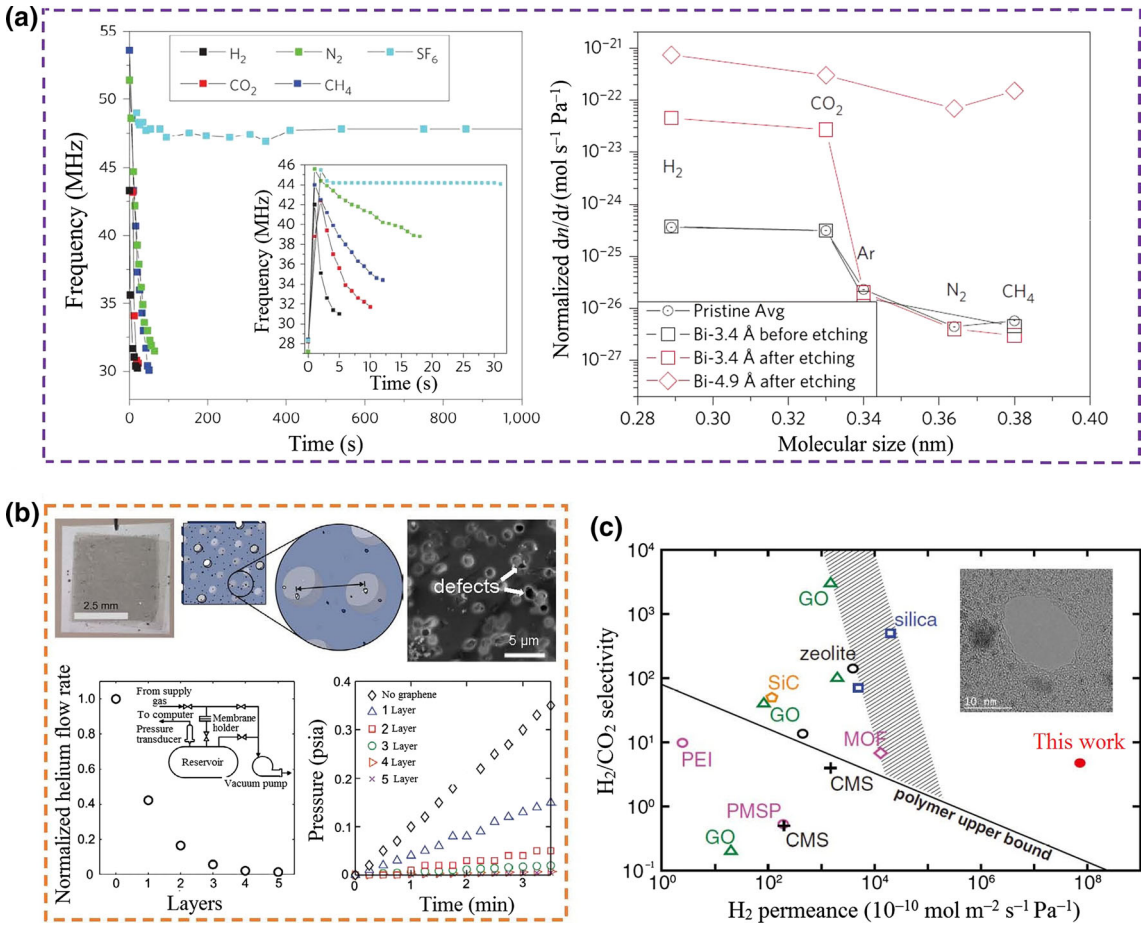

Fig. 3 (Color online) Experimental works on NPG membranes for gas separation. **a** Transport rates measurement for various gases in a NPG membrane using mechanical resonance. Reprinted with permission from Ref. [25], Copyright 2012, Nature Publishing Group. **b** Gas flow rates through the single-layer and multi-layer graphene with intrinsic defects. Reprinted with permission from Ref. [87], Copyright 2014, American Chemical Society. **c** Comparison of H_2/CO_2 gas separation performances among the NPG membrane (7.6-nm pore diameter, with 4.0 % porosity) and other membranes. Reprinted with permission from Ref. [56], Copyright 2014, American Association for the Advancement of Science

realized in spite of the presence of non-selective defects. This study further promoted the realization of practical and high-quality NPG-based gas separation membranes. Kim et al. [88] also examined the role of defects on the gas transport through NPG membranes and showed that the gas permeability decreased gradually with increasing the number of graphene layers. At the same time, they found that the O_2/N_2 selectivity improved with increasing the graphene stacking, suggesting that the gases diffused not only through the defects on the graphene sheet but also between the graphene inter-layers.

Recently, Celebi et al. [56] measured the transport rates of gas, liquid, and water vapor across physically perforated double-layer graphene, possessing a few million pores with narrowly distributed diameters between <10 nm and 1 μm. Their measured transport rates were in agreement with the predictions of 2D transport theories. They showed that the permeance of the NPG membranes far exceeded those of the polymer membranes with a finite thickness (Fig. 3c). It is noted that the area of their fabricated membrane was up to millimeter squares, which can be employed in the real industrial applications. The experimental works on the NPG membranes with large area, high-density pores and few defects are expected. We believe that more and more experimental works on NPG membranes accompanying advanced fabrication technologies will be launched, and the NPG-based membrane is becoming a reality.

3 Water purification

3.1 Theoretical work

Both the theoretical and experimental works on the NPG membranes for water purification are limited comparing to

those of gas separation, because the conception of water purification NPG membrane was proposed later. Cohen-Tanugi and Grossman [57] firstly demonstrated that the single-layer graphene with nanometer-scale pores can be used as an effective membrane for water desalination (Fig. 4a). The desalination performance of the graphene was mainly dominated by the pore size, chemical functionalization, and applied pressure, in which the pore diameter played a crucial role for the salt rejection. Meanwhile, the hydroxyl groups added to pore rim can greatly increase the water flux owing to their hydrophilicity. They showed that the water permeability was several orders of magnitude higher than those of conventional reverse osmosis membranes. Konatham et al. [89] also studied the separation of water and ions via graphene nanopores by using MD simulations. They found that the nanopores of diameter $\approx$7.5 Å can effectively exclude ions and the nanopores modified by carboxyl groups exhibited higher ion exclusion. All of above showed that the NPG has tremendous promise as a high-efficiency membrane for water purification by creating specific nanopores with appropriate sizes, geometries, and chemical modifications. For such ultrapermeable membranes, Cohen-Tanugi et al. [90] theoretically showed that a tripling in water permeability resulted in a 44 % fewer pressure requirement or 15 % less energy consumption for a seawater reverse osmosis plant and a 63 % fewer pressure requirement or 46 % less energy consumption for brackish water. It is noted that the MD simulation system for water transport through the NPGs is different from that for the gas transport. In the water transport systems, usually a rigid piston is employed to slowly push the water solutions toward the NPG membranes under a given pressure [57, 91–94].

To be more confident for the application of NPG membranes in water purification, Cohen-Tanugi and Grossman [94] further demonstrated that the NPG membranes can maintain ultrahigh water permeability even at

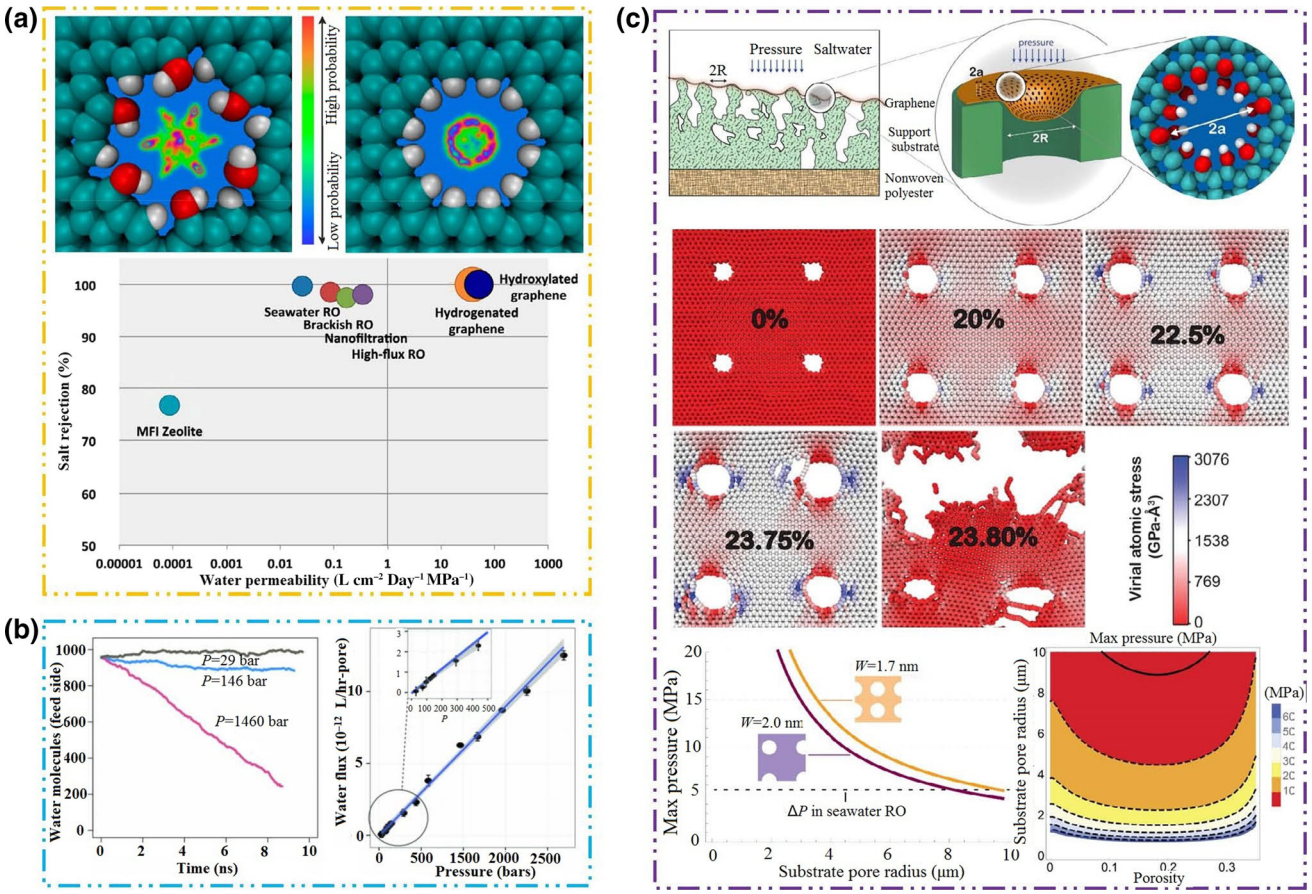

Fig. 4 (Color online) Theoretical works on NPG membranes for water purification. **a** Two different nanopores functionalized by H and -OH, and the water desalination performance of NPG membranes. Reprinted with permission from Ref. [57], Copyright 2012, American Chemical Society. **b** Molecular permeation number and water flux for the NPG water desalination membranes at low pressures. Reprinted with permission from Ref. [94], Copyright 2014, American Institute of Physics. **c** Mechanical strength of NPG membranes supported by porous substrates for the application of water desalination reverse osmosis system. Reprinted with permission from Ref. [95], Copyright 2014, American Chemical Society

low pressures, closing to the realistic pressures in the real reverse osmosis systems (Fig. 4b). Using MD simulations and continuum fracture mechanics, they also revealed that the NPG membranes were strong enough to maintain their integrities under the high hydraulic pressures inherent to the reverse osmosis systems (Fig. 4c) [95]. They showed that an appropriate porous substrate with holes smaller than 1 μm allowed the NPG membranes to resist a pressure exceeding 57 MPa (ten times higher than the typical pressures in the seawater reverse osmosis systems). In addition, they found that the NPG membranes with higher porosity may resist even higher pressures.

Actually, before the demonstration of NPG as an efficient water purification membrane, several works have been conducted on the permeation of ions and water through graphene nanopores, respectively. Sint et al. [39] using MD simulations showed that the graphene with functionalized nanopores can serve as the high ions sieves with high transport rates. Hu et al. [96] quantified the importance of the hydrodynamic transport, thermal fluctuations, and electric pressure on the transport of Na^+ and Cl^- ions in an electric field. They also found that the water permeated through the nanopore with an average velocity proportional to the applied voltage and a flux independent on the pore diameter. For water, Suk and Aluru [93] found that the NPG membranes with big pores can provide higher water flux than carbon nanotubes, while for the NPG membranes with small pores, they exhibited lower water flux comparing to carbon nanotubes. Recently, several works were also conducted on the permeation of ions and water. Zhu et al. [92] indicated that the water flux of the pores with a diameter $\geq$15 Å exhibited a linear dependence on the pore area, while for the small pores a nonlinear relationship between the water flux and the pore area appeared. Suk and Aluru [97] investigated the static and dynamic properties of ions in the graphene nanopores using MD simulations. As the pore radius smaller than 0.9 nm, ion concentration and mobility in the graphene nanopores decreased sharply owing to the liquids with layered structure in the pore-axial direction. Zhao et al. [98] investigated the selective ion transport in the KCl solutions through the charge-modified graphene nanopores under an external electric field. They showed that the ion selectivity greatly depended on the pore size and the charges on the pore edge. A complete rejection of Cl^- can be realized with appropriate pore diameter and electric charge. The investigations on the transport of water and ions through graphene nanopores are very crucial for the understanding of the mechanisms of water purification using NPG membranes. Thus, these studies are very important for the application of NPG membranes in water purification. More relevant studies are urgently needed.

3.2 Experimental work

There are only several works focusing on the experimental measurements of the water and ion transport through NPG membranes. Because the intrinsic defects in graphene would affect the performance of NPG membranes, O'Hern et al. [33] firstly evaluated the effect of defects in the chemical vapor deposition graphene on the permeation of several molecules and ions. They transferred a single-layer graphene onto a porous polycarbonate substrate to prepare the graphene membranes of areas more than 25 mm^2. They found a size-selective transport of different molecules through the graphene membranes with intrinsic defective pores of diameter 1–15 nm. In the practical NPG membranes, particular nanopores should be created artificially. Therefore, subsequently they purposefully produced the nanopores in the graphene by ion bombardment and oxidative etching (Fig. 5a) [58]. A serial of pores of diameter $\approx$0.40 nm and density exceeding 10^{12} cm^{-2} were generated. The transport rate measurements showed that at short oxidation times, the pores were cation-selective, agreeing with the electrostatic repulsion from negatively charged functional groups. While at long oxidation times, the pores allowed the transport of salt but prevented the transport of a larger organic molecule due to steric size exclusion. Their work demonstrated that the pore sizes can be tuned by changing the etching time, which provided a great opportunity for the development of NPG membranes. In Ref. [56], the measurement of water transport rate through the NPGs was also performed. Thanks to its atomic thickness, the fabricated NPG membranes showed higher permeance of water comparing to the other ultrafiltration membranes, highlighting the ultimate permeation of the NPG membranes.

Recently, the experimental measurements for the water desalination were conducted by Surwade et al. [59] and O'Hern et al. [99], respectively. Surwade et al. [59] designed a desalination experimental system and measured the water flux of a NPG membrane (Fig. 5b). The NPG membrane was synthesized based on the ambient-pressure chemical vapor deposition graphene on a copper foil. They created the tunable nanometer-sized pores using the oxygen plasma etching processes. This NPG membrane showed the high selectivities of water molecule over dissolved ions (K^+, Na^+, Li^+ and Cl^-) and possessed a nearly 100 % salt rejection rate and a high water transport rate. O'Hern et al. [99] fabricated a centimeter squares defect-free NPG membrane by blocking the intrinsic defects in the pristine graphene using a multiscale leakage-sealing process (Fig. 5c). This membrane exhibited the excellent rejection ability of multivalent ions and small molecules accompanying with high water permeation rates. All of

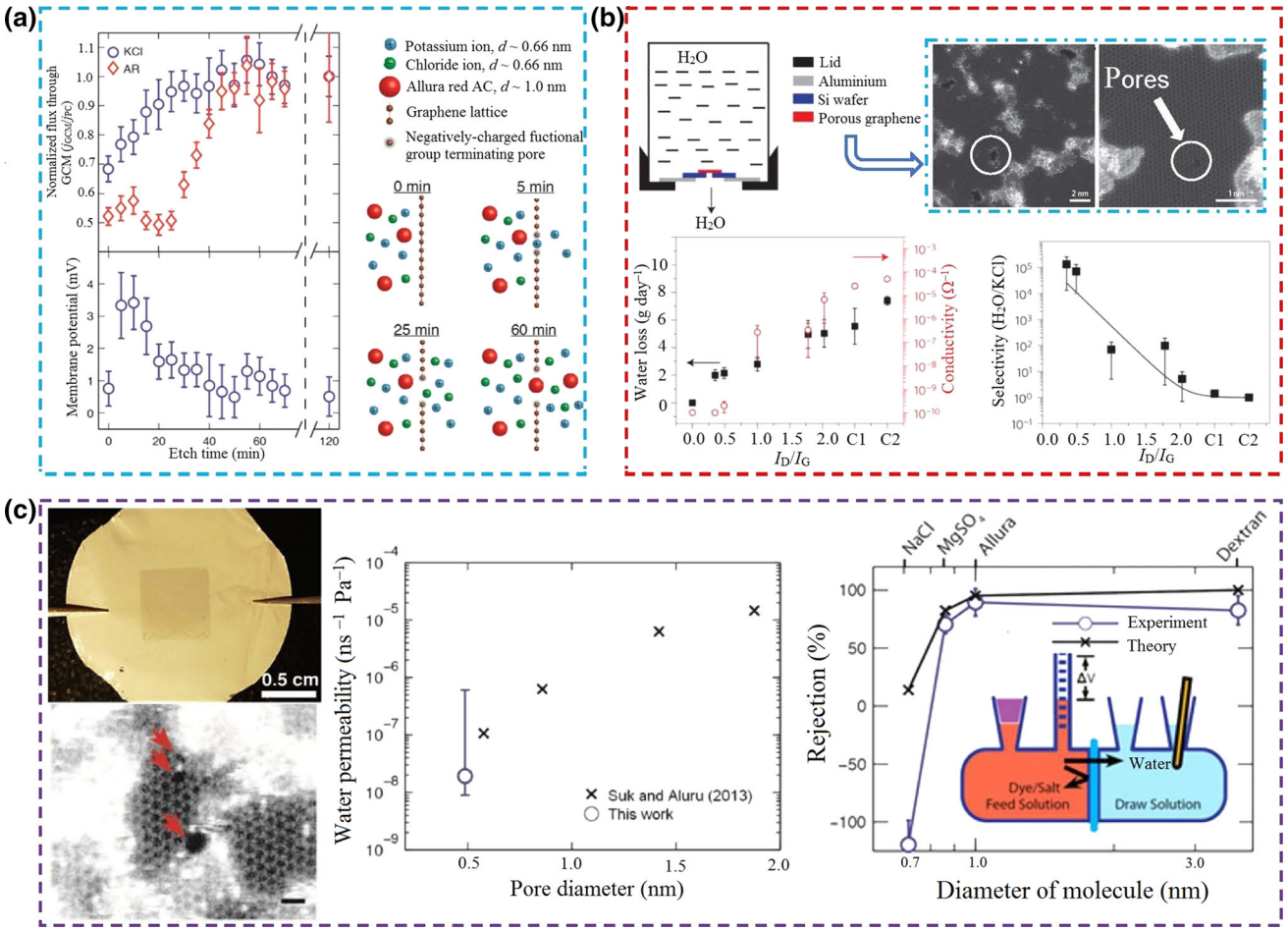

Fig. 5 (Color online) Experimental works on NPG membranes for water purification. **a** Diffusive flux through the graphene membrane and its potential measurements. Reprinted with permission from Ref. [58], Copyright 2014, American Chemical Society. **b** Water loss and ionic conductivity through the NPG membranes and their water/salt selectivity. Reprinted with permission from Ref. [59], Copyright 2015, Nature Publishing Group. **c** Water permeability and salt rejection comparison between the MD simulations and the theoretical continuum model. Reprinted with permission from Ref. [99], Copyright 2015, American Chemical Society

these advanced works offered a proof that the NPG membranes can serve as a novel and high-efficiency membrane for water purification applications. Apart from the transport of water and ions, the transport of other substances necessarily appears in the water purifications, such as the trihalomethanes [100]. Thus, the permeation of kinds of substances through the NPGs is expected to be explored by the researchers.

4 Molecular permeation mechanism

4.1 Gas separation

Although many studies have identified extremely high mass transport rates through the NPG membranes, how the molecules transport through the nanopores in graphene remains unclear. Until now, to our knowledge a few studies were involved to investigate the mechanisms of gas molecular permeation through the NPG membranes. Drahushuk and Strano [82] identified five rate-limiting steps for a gas molecular transport through the graphene nanopores, i.e., the gas molecule adsorbed onto the graphene surface (step 1), the molecule diffused to the pore and associated into the potential well positioned above the pore (step 2), the molecule passed through the pore (step 3), the molecule disassociated from the pore area to the graphene surface (step 4), and the molecule desorbed from the surface and entered the gas phase (step 5) (Fig. 6a). Then, they derived the analytical expressions for the gas fluxes at these rate-limiting steps for several graphene pores. Based on the molecular adsorption layer on the graphene surface, Sun et al. [78] broke down the gas molecular motion in the NPG membranes into four cases (Fig. 6b) and concluded that a molecular crossing event happened only if it moved from the bulk phase on one side to the bulk phase on the

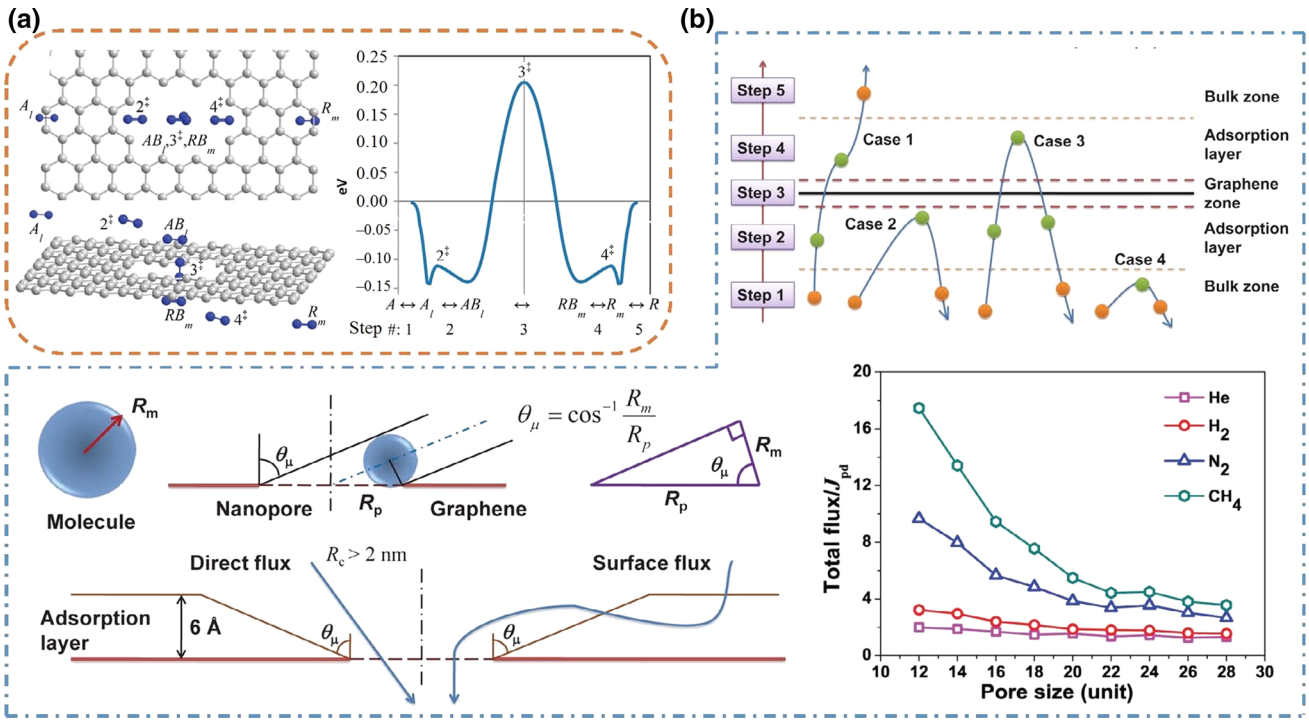

Fig. 6 (Color online) Gas molecular permeation mechanisms through NPG membranes. **a** Five rate-limiting steps for N_2 passing through a graphene pore. Reprinted with permission from Ref. [82], Copyright 2012, American Chemical Society. **b** Typical molecular transport modes in a NPG membrane and the molecular permeation regimes, i.e., direct flux and surface flux. Reprinted with permission from Ref. [78], Copyright 2014, American Chemical Society

other side of the membrane. Moreover, they proposed two mechanisms (direct mechanism versus surface mechanism) for the molecular permeation through the NPG membranes (Fig. 6b). In the direct flux, the molecules crossed directly from the bulk phase on one side of the graphene to the bulk phase on the other side; in the surface flux, the molecules crossed after being adsorbed onto the graphene surface. They found that the surface flux of weakly adsorbed gases (e.g., He and H_2) was negligible, while that of strongly adsorbed gases (e.g., CH_4 and N_2) was very appreciable. Meanwhile, they quantified the relative contribution of the direct and surface mechanisms and showed that the direct flux can be predicted using the kinetic theory with an appropriate modification considering the steric pore–molecule interactions. In the ideal gas kinetic theory, the flux of point particles through a certain area can be obtained by

$$J = \frac{P_g}{\sqrt{2\pi RMT}}, \tag{3}$$

where T is the temperature, P_g is the gas pressure, R is the universal gas constant, M is the molar mass. However, for the gas molecules with a certain size, the direct flux J_{pd} should be obtained after a reduction $\delta(R_p/R_m)$ in the ideal gas flux J, as follows

$$J_{pd} = J \cdot \delta(R_p/R_m). \tag{4}$$

In their work, they assumed that the reduction in molecular flux was completely steric considerations, and the gas molecules behaved as hard spheres of known kinetic diameters. Therefore, the reduction coefficient $\delta(R_p/R_m) \leq 1$, and it was calculated via the fraction of trajectories with molecular centers intersecting with the pore rim graphene atoms. The surface flux is related to the molecular diffusion on the graphene surface, and thus a diffusion model coupling with appropriate boundary conditions and Fick law can be established to predict the surface flux. Until now, the transport of gas molecules through the NPG membranes can basically realize the mathematical description.

4.2 Water purification

For the water purification by NPG membranes, several studies reported the microscopic mechanisms of water and ion transport through the graphene nanopores. Zhu et al. [92] showed that the continuum water flow in big graphene

pores transitioned to discrete molecular flow patterns in small pores. For the small graphene pores comparable to molecular size, the water flow rate was strongly affected by the microstructure of the water molecules in the pore; while for the big pores, the water flow rate can be predicted by the conventional theoretical models because the pore edge region was negligible. Suk and Aluru [93] demonstrated that for the big graphene pores, where the water structure was not single file, the NPG membranes provided higher water flux compared with carbon nanotube membranes (Fig. 7a). They explained the results through a detailed analysis on the pressure distribution, velocity profiles, and potential of mean force. In the water purification, the ion transports are always involved. Konatham et al. [89] indicated that the ions can be excluded using a non-functionalized pore of diameter ~7.5 Å, whereas the ions can easily permeate through the pores of diameters ~10.5 and 14.5 Å (Fig. 7b). The carboxyl groups on the pore rim can effectively enhance the ions exclusion efficiency at low ion concentrations and small pore diameters. Sint et al. [39] modeled the passage of hydrated ions through the N-, F-, and H-functionalized graphene nanopores (Fig. 7c). They found that the nanopores modified by negatively charged N and F atoms preferred the crossing of cations, while the nanopores modified by positively charged H atoms favored the crossing of anions. Zhao et al. [98] revealed that the negative charges on the pore edge can effectively hinder the passage of Cl^- while enhance the passage of K^+. Kang et al. [101] indicated that the Na^+ and K^+ ion selectivity of graphene nanopores was determined by their sizes. They found that the free energy barrier of smaller Na^+ was significantly higher than that of K^+ in the nanopores with a certain size and observed a high Na^+ and K^+ ion selectivity of the nanopores with a distance about 3.9 Å between two neighboring O atoms.

Although the influencing factors are identified, the transport modes of water molecules and corresponding analytical models are missing. Theoretical models are urgently anticipated to predict the permeation flux of water through the two-dimensional graphene nanopores with different sizes. The water flux through the NPG membranes may be obtained based on the Hagen–Poiseuille equation

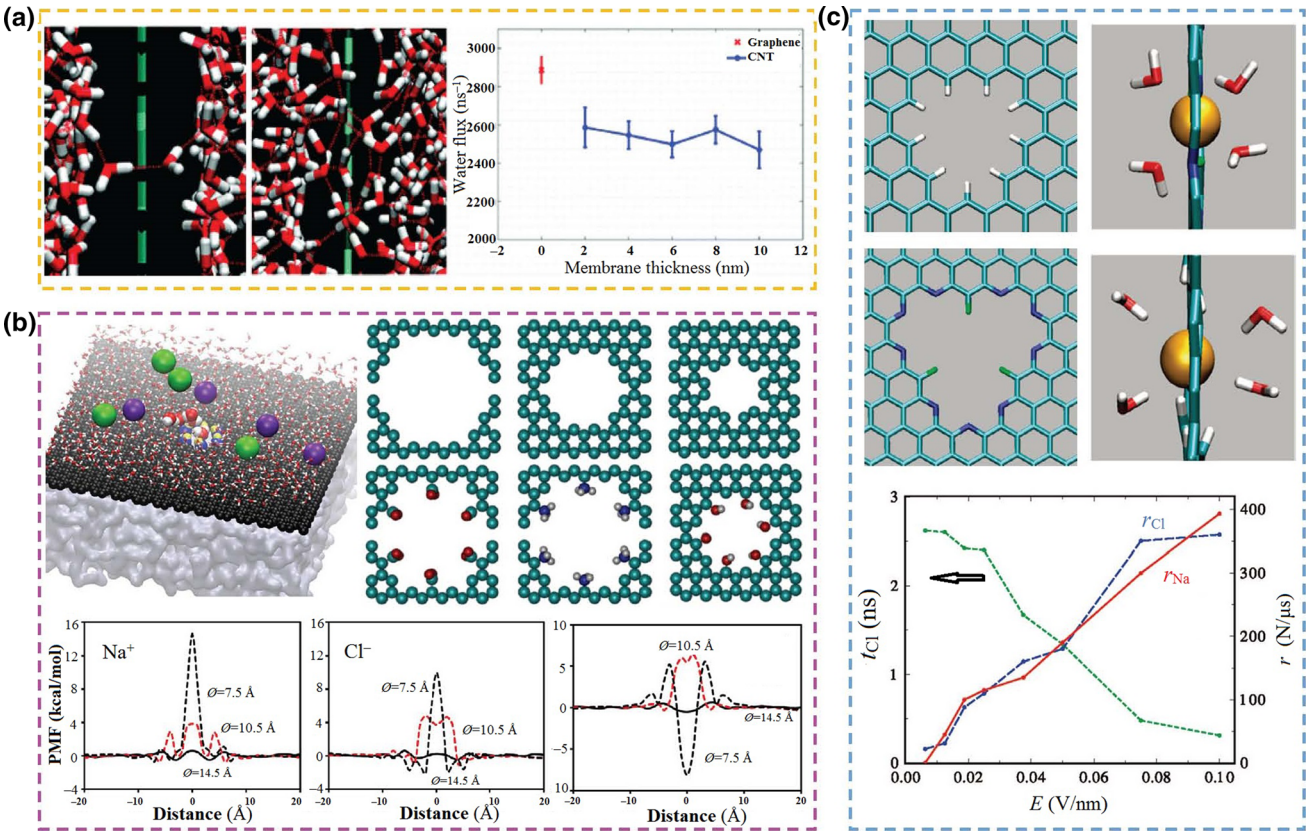

Fig. 7 (Color online) Water and ion transport through NPG membranes. **a** Water structure in the nanopore during the permeation process through the NPGs. Reprinted with permission from Ref. [93], Copyright 2010, American Chemical Society. **b** Ion and water transport through the graphene nanopores with different sizes and functionalizations. Reprinted with permission from Ref. [89], Copyright 2013, American Chemical Society. **c** Ion transport through the graphene nanopores functionalized by N, F, and H atoms. Reprinted with permission from Ref. [39], Copyright 2008, American Chemical Society

with a modification considering the velocity slip and entrance/exit pressure loss etc. The expression of the Hagen–Poiseuille equation is

$$Q = \frac{\pi R^4 \Delta P}{8\mu L}, \quad (5)$$

where Q is the volumetric flow rate, P is the pressure drop, R is the pore radius, μ is the water viscosity, and L is the membrane thickness. The analytical models for the transport of ions are more difficult to be developed, because of the appearance of the electrostatic interactions etc.

5 Fabrication of NPG membrane

5.1 Graphene transfer

In the fabrication of NPG membranes, the transfer of graphene to a suitable porous substrate and the generation of nanopores in the graphene are two main processes. The graphene transfer process is especially necessary for the top-down NPG fabrication methods. Due to the rapid development in this field, we just summarize some representative methods to highlight the importance of the fabrication of NPG-based membranes. In the graphene transfer process, no damage on the graphene is expected. Until now, several advanced graphene transfer methods were developed. The graphene transfer method varies with the fabrication method of graphene itself. For the mechanically exfoliated graphene, in the method developed by Liang et al. [102], the stamp with an adhering layer was pressed on highly oriented pyrolytic graphite, and the patterned portion of the stamp brought graphene with it. Then, the graphene was stuck to the substrate by pressing the stamp-supported graphene. Liu and Yan [103] bonded a silicon wafer to the graphene after a chemical modification with peruorophenylazide. Reina et al. [104] transferred the chemical vapor deposition graphene to an arbitrary substrate. They firstly spin-coated and cured a 1-μm layer of polymethyl(methyl) acrylate on the graphene (Fig. 8a). Then, the substrate-supported graphene was fabricated after the etching, air-dry, and dissolution processes. Regan et al. [105] directly transferred the low-pressure chemical vapor deposition graphene to a TEM grid with holes of diameter 1.2 μm. They filled isopropanol in the gaps between the TEM grid and the graphene, which helped them contact with each other during the evaporation process. Caldwell et al. [106] developed a dry transfer technique for the epitaxial graphene from the C-face of 4H-SiC onto the SiO_2, GaN, and Al_2O_3 substrates using a thermal release tape. Allen et al. [107] developed a procedure to transfer the chemically modified graphene by using a polydimethylsiloxane tamp and conducting the surface energy manipulation (Fig. 8b). Actually, many other graphene transfer methods are currently being developed very well in the material science, which will promote the rapid development of the NPG-based separation membranes.

In the experimental studies on the NPG membranes for the applications of gas separation and water purification, some advanced graphene transfer methods were also developed. In the work by O'Hern et al. [33], a transfer process of the chemical vapor deposition graphene to a porous polycarbonate track etch support was developed. They firstly etched the back sides of the copper foil with graphene grown by the chemical vapor deposition in an ammonium persulfate solution to expose the copper and reduce the foil thickness. After a rinsing step, they pressed the graphene on the copper foil to a larger supporting substrate. Then, they completely removed the remaining copper foil using an ammonium persulfate solution. Finally, a rinsing process in ethanol and an air-drying process were done. More layers of graphene can be transferred by mechanically pressing the graphene with copper foil onto the substrate with transferred graphene, accompanying with the etching, rinsing, and drying processes [87]. In Ref. [56], Celebi et al. modified the transfer method developed by Suk et al. [108]. They spined the polymethyl methacrylate (PMMA) on the as-grown graphene to yield the PMMA/graphene/copper polymer layers. Then, they etched the copper using a $(NH_4)_2S_2O_8$ solution and rinsed the PMMA/graphene layer in a water bath. Finally, the PMMA was removed in a quartz tube furnace at 400 °C for 2 hours. Anyway, the graphene transfer can be well realized using various methods. In the future, more concerns should be paid on the damages of the graphene during the transfer process, because the qualities of the transferred graphene are very important for the membrane fabrication.

5.2 Nanopore generation

The pore generation is essentially important for the permeability and selectivity of the NPG-based membranes. For the pore generation in the graphene, the top-down and bottom-up methods were both well developed, where the top-down methods were developed prior to the bottom-up methods. The top-down methods mainly include electron-beam irradiation [109], ion beam bombardment [34], ultraviolet-induced oxidative etching [25, 37, 38], oxygen plasma etching [59], block copolymer lithography [35], and nanosphere lithography [110]. In 2008, Fischbein and Drndić [109] demonstrated that the pores can be generated in the suspended multilayer graphene sheets by the controlled exposure to a focused electron-beam irradiation using a TEM at room temperature (Fig. 9a). In this technique, stable nanopores can be generated in a graphene

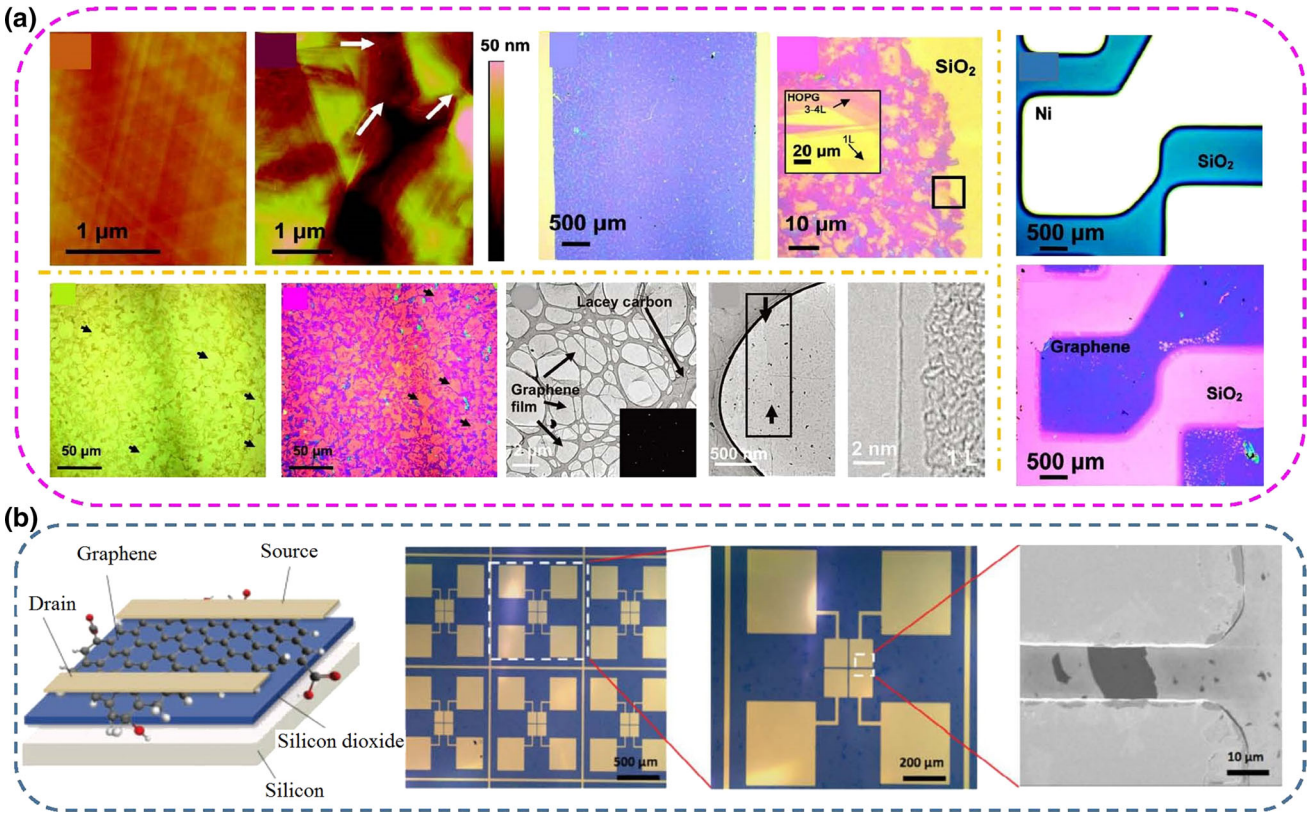

Fig. 8 (Color online) Methods of graphene transfer to porous substrates. **a** Transfer of graphene fabricated via ambient-pressure chemical vapor deposition on polycrystalline Ni films to the arbitrary substrates. Reprinted with permission from Ref. [104], Copyright 2009, American Chemical Society. **b** Schematic and SEM of the fabricated graphene device by a transfer process. Reprinted with permission from Ref. [107], Copyright 2009, Wiley Online Library

sheet within a few seconds. To successfully generate the nanopores, the energy of electron should reach up to hundreds of keV. However, Russo and Golovchenko [34] showed that the combination of ion beam bombardment and low-energy defocused electron beam was able to effectively generate nanopores in the graphene sheet (Fig. 9b). They firstly created some nucleation sites by a bombardment with 3 keV argon ions and then generated the nanopores by enlarging the nucleation sites using a uniform defocused electron beam of only 80 keV. Ultraviolet-induced oxidative etching can also generate nanopores in the graphene, and Koenig et al. [25] used this method to create pores in the micrometer-sized graphene membranes and showed that the resulted membranes can be used as molecular sieves. Liu et al. [38] found that the oxygen etching kinetics varied significantly with the number of graphene layers. For example, the three-layer graphene exhibited an etching performance similar to the graphite, while the single-layer graphene reacted faster with random etch pits (Fig. 9c). Surwade et al. [59] created the nanometer-sized pores in a monolayer graphene using an oxygen plasma etching process. In this process, the size of the pores can be tuned. Actually, there are some other etching methods [4, 39, 111, 112], which are all effective for creating nanopores. O'Hern et al. [58] firstly introduced isolated reactive defects in the graphene via an ion bombardment and subsequently enlarged them by oxidative etching into permeable pores of diameters (0.40 ± 0.24) nm. In order to fabricate the large-area NPG membranes, the lithography methods were introduced. In 2010, Bai et al. [35] reported the fabrication of NPG membranes by the block copolymer lithography. Then, Safron et al. [110] developed the nanosphere lithography, which was a complementary technique to the block copolymer lithography. In addition, the nanoimprint lithography can also fabricate the NPG membranes combined with the block copolymer self-assembly [113]. At the same time, NPG membranes can be fabricated through various chemical or photocatalytic approaches; for the details one can see Ref. [114].

In the top-down method, the generated nanopores usually have rough and disordered edges, which are not good for the molecular transport. Thus, the bottom-up methods are expected. Safron et al. [115] firstly demonstrated a bottom-up method called as barrier-guided chemical vapor deposition, which relied on the self-terminating growth

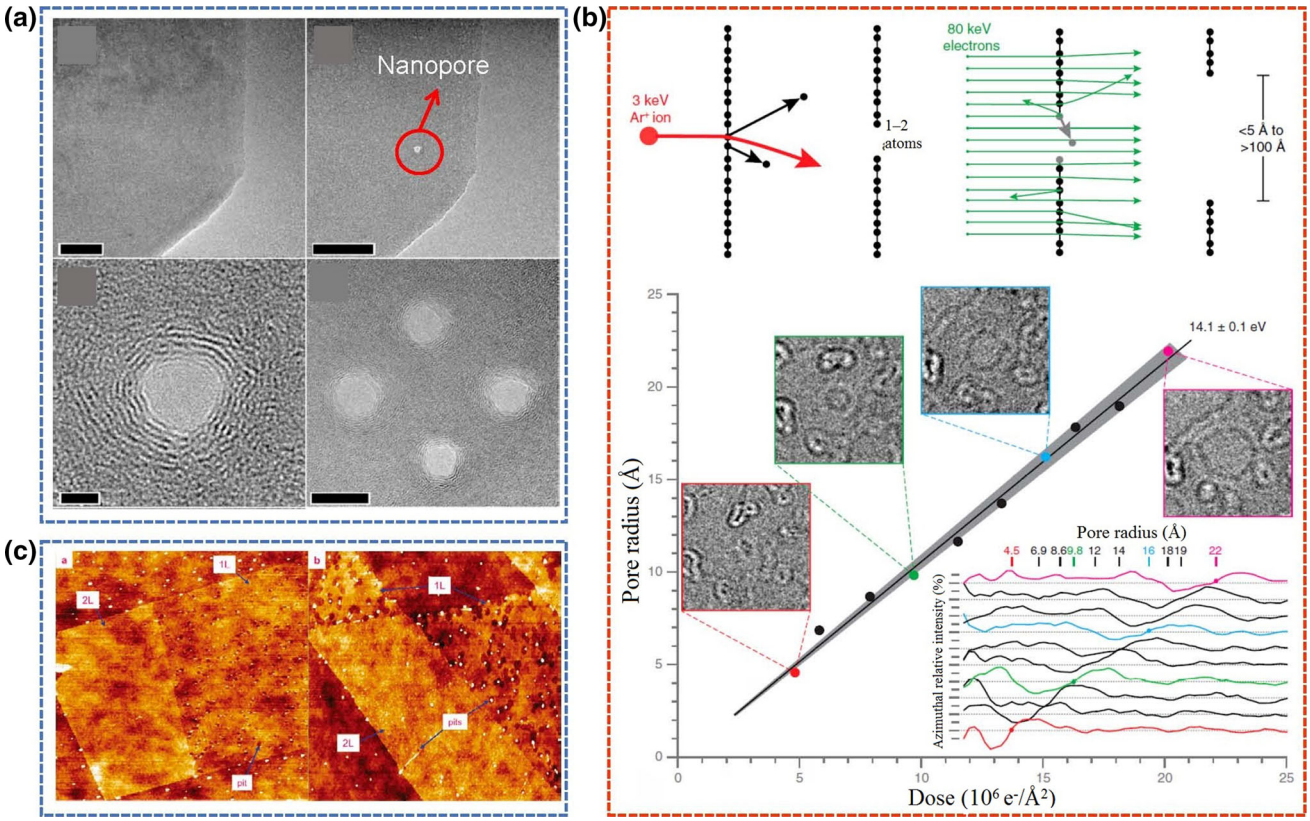

Fig. 9 (Color online) Methods of nanopore generation in graphene membrane. **a** TEM images before and after the nanopore generation in a suspended graphene sheet by electron-beam irradiation. Reprinted with permission from Ref. [109], Copyright 2008, American Institute of Physics. **b** Diagram of the graphene nanopore fabrication process and its growth trajectories. Reprinted with permission from Ref. [34], Copyright 2012, National Academy of Sciences of the United States of America. **c** AFM images of oxidized single-layer and double-layer graphene. Reprinted with permission from Ref. [38], Copyright 2008, American Chemical Society

process. Al_2O_3 was employed as an inert barrier, and the CH_4 molecules were decomposed on the exposed copper to form a carbon layer. A patterned barrier layer terminated the growth of graphene in the selected areas of the copper substrate, resulting in a NPG with controlled placement, orientation, spatial, and lateral extent. Several other bottom-up methods have also been developed [116–118]. In Ref. [117], the porous copper foil patterned by nanospheres, was directly used as a substrate for the graphene growth. Comparing to the top-down methods, the bottom-up methods are limited and much efforts should be done to fabricate high-quality large-area NPG membranes.

6 Conclusions and outlook

We have highlighted the recent advances in the NPG membranes for gas separation and water purification. We summarized the advanced theoretical and experimental works on the NPG membranes with a major emphasis on the gas/water molecular transport mechanisms as well as their fabrication methods. We anticipate that this review can provide the state-of-the-art advancements at the forefront of the research field, and it is a good start to make the NPG membrane a reality in the near future.

As Koh and Lively [119] noted, there are many challenges to be addressed before such membranes could be of practical use, including the mechanical stability under high flow shear rates and pressure, the supporting of large continuous sheets of graphene in a membrane module, the scalable nanopore generation in the graphene and other issues, such as membrane fouling, concentration polarization, and pore blocking by the salt ions. Despite facing these challenges, the practical NPG membranes are becoming a reality. More works are urgently anticipated to promote the application of NPG membranes in industry. In Fig. 10, we show the issues must be addressed before the NPG membrane becomes a reality and the outlook of its development. Firstly, the mechanisms of molecular permeation through the NPG membranes should be made clear from theoretical points of view. The transport regimes of gas/water molecules, ions, and other substances through the

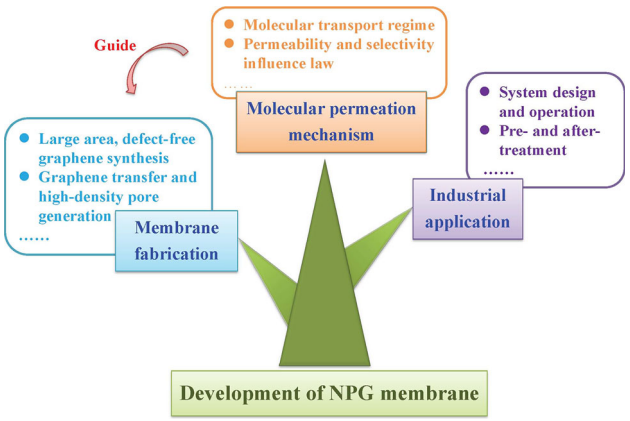

Fig. 10 (Color online) Outlook of the development of NPG membranes. Molecular permeation mechanism, membrane fabrication technology, and industrial application research are three key issues that must be addressed to promote the development of NPG membranes

NPGs are expected to be identified to exactly show how these substances permeate through the two-dimensional graphene nanopores. The influencing factors of the permeability/selectivity of the NPG membranes and their influencing mechanisms and laws should be widely investigated. These investigations can help the researchers and engineers find the optimal NPG membrane constitution, pore structure, and size, etc. Secondly, the advanced NPG membrane fabrication technologies must be well developed. The design of NPG membranes should be guided and conducted on the basis of the understanding of molecular permeation mechanisms. In the industrial applications, the large-area defect-free NPG membranes with high-density sub-nanometer pores are preferable. Hence, the large-area defect-free graphene synthesis, high-quality graphene transfer, and high-density pore generation methods should be paid more attentions. Thirdly, the application research must be conducted for the industrial applications of the NPG membranes. For the NPG membranes, their operation system should differ from the systems for the conventional separation membranes, owing to the special issues related to the NPG membranes, such as the porous supports with micrometer-sized holes. "How to design and operate the NPG membrane separation system ?", "What should do before and after the operation of the system ?" and other questions must be answered to ensure the high-efficiency application of the NPG membranes.

Acknowledgments This work was supported by the National Natural Science Foundation of China (51425603 and 51236007).

Conflict of interest The authors declare that they have no conflict of interest.

References

1. Allen MJ, Tung VC, Kaner RB (2010) Honeycomb carbon: a review of graphene. Chem Rev 110:132–145
2. Geim AK (2009) Graphene: status and prospects. Science 324:1530–1534
3. Meyer JC, Geim AK, Katsnelson MI et al (2007) The structure of suspended graphene sheets. Nature 446:60–63
4. Girit CO, Meyer JC, Erni R et al (2009) Graphene at the edge: stability and dynamics. Science 323:1705–1708
5. Fasolino A, Los JH, Katsnelson MI (2007) Intrinsic ripples in graphene. Nat Mater 6:858–861
6. Balandin AA, Ghosh S, Bao WZ et al (2008) Superior thermal conductivity of single-layer graphene. Nano Lett 8:902–907
7. Chen SS, Wu QZ, Mishra C et al (2012) Thermal conductivity of isotopically modified graphene. Nat Mater 11:203–207
8. Yao WJ, Cao BY (2014) Thermal wave propagation in graphene studied by molecular dynamics simulations. Chin Sci Bull 59:3495–3503
9. Lee C, Wei XD, Kysar JW et al (2008) Measurement of the elastic properties and intrinsic strength of monolayer graphene. Science 321:385–388
10. Gómez-Navarro C, Burghard M, Kern K (2008) Elastic properties of chemically derived single graphene sheets. Nano Lett 8:2045–2049
11. Geim AK, Novoselov KS (2007) The rise of graphene. Nat Mater 6:183–191
12. Castro Neto AH, Guinea F, Peres NMR et al (2009) The electronic properties of graphene. Rev Mod Phys 81:109–162
13. Bolotin KI, Sikes KJ, Jiang Z et al (2008) Ultrahigh electron mobility in suspended graphene. Solid State Commun 146:351–355
14. Novoselov KS, Falko VI, Colombo L et al (2012) A roadmap for graphene. Nature 490:192–200
15. Hu S, Lozada-Hidalgo M, Wang FC et al (2014) Proton transport through one-atom-thick crystals. Nature 516:227–230
16. Achtyl JL, Unocic RR, Xu L et al (2015) Aqueous proton transfer across single-layer graphene. Nat Commun 6:6539
17. Bunch JS, Verbridge SS, Alden JS et al (2008) Impermeable atomic membranes from graphene sheets. Nano Lett 8:2458–2462
18. Berry V (2013) Impermeability of graphene and its applications. Carbon 62:1–10
19. Tsetseris L, Pantelides ST (2014) Graphene: an impermeable or selectively permeable membrane for atomic species? Carbon 67:58–63
20. Xu P, Yang J, Wang K et al (2012) Porous graphene: properties, preparation, and potential applications. Chin Sci Bull 57:2948–2955
21. Liu Y, Chen X (2014) Mechanical properties of nanoporous graphene membrane. J Appl Phys 115:034303
22. Anonymous (2015) Graphene opens up to new applications. Nat Nanotechnol 10:381
23. Du HL, Li JY, Zhang J et al (2011) Separation of hydrogen and nitrogen gases with porous graphene membrane. J Phys Chem C 115:23261–23266
24. Jiang DE, Cooper VR, Dai S (2009) Porous graphene as the ultimate membrane for gas separation. Nano Lett 9:4019–4024
25. Koenig SP, Wang LD, Pellegrino J et al (2012) Selective molecular sieving through porous graphene. Nat Nanotechnol 7:728–732
26. Wen BY, Sun CZ, Bai BF (2015) Molecular dynamics simulation of the separation of CH_4/CO_2 by nanoporous graphene. Acta Phys Chim Sin 31:261–267

27. Kim KS, Zhao Y, Jang H et al (2009) Large-scale pattern growth of graphene films for stretchable transparent electrodes. Nature 457:706–710
28. Li XS, Cai WW, An JH et al (2009) Large-area synthesis of high-quality and uniform graphene films on copper foils. Science 324:1312–1314
29. Novoselov KS, Geim AK, Morozov SV et al (2004) Electric field effect in atomically thin carbon films. Science 306:666–669
30. Park S, Ruoff RS (2009) Chemical methods for the production of graphenes. Nat Nanotechnol 4:217–224
31. Aleman B, Regan W, Aloni S et al (2010) Transfer-free batch fabrication of large-area suspended graphene membranes. ACS Nano 4:4762–4768
32. Lin YC, Jin CH, Lee JC et al (2011) Clean transfer of graphene for isolation and suspension. ACS Nano 5:2362–2368
33. O'Hern SC, Stewart CA, Boutilier MSH et al (2012) Selective molecular transport through intrinsic defects in a single layer of CVD graphene. ACS Nano 6:10130–10138
34. Russo CJ, Golovchenko JA (2012) Atom-by-atom nucleation and growth of graphene nanopores. Proc Natl Acad Sci USA 109:5953–5957
35. Bai JW, Zhong X, Jiang S et al (2010) Graphene nanomesh. Nat Nanotechnol 5:190–194
36. Bieri M, Treier M, Cai JM et al (2009) Porous graphenes: two-dimensional polymer synthesis with atomic precision. Chem Commun 45:6919–6921
37. Huh S, Park J, Kim YS et al (2011) UV/Ozone-oxidized large-scale graphene platform with large chemical enhancement in surface-enhanced raman scattering. ACS Nano 5:9799–9806
38. Liu L, Ryu SM, Tomasik MR et al (2008) Graphene oxidation: thickness-dependent etching and strong chemical doping. Nano Lett 8:1965–1970
39. Sint K, Wang B, Kral P (2008) Selective ion passage through functionalized graphene nanopores. J Am Chem Soc 130:16448
40. Huang K, Liu G, Lou Y et al (2014) A graphene oxide membrane with highly selective molecular separation of aqueous organic solution. Angew Chem Int Ed 53:6929–6932
41. Huang H, Mao Y, Ying Y et al (2013) Salt concentration, pH and pressure controlled separation of small molecules through lamellar graphene oxide membranes. Chem Commun 49:5963–5965
42. Shen J, Liu G, Huang K et al (2015) Membranes with fast and selective gas-transport channels of laminar graphene oxide for efficient CO_2 capture. Angew Chem Int Ed 54:578–582
43. Huang H, Song Z, Wei N et al (2013) Ultrafast viscous water flow through nanostrand-channelled graphene oxide membranes. Nat Commun 4:2979
44. Ying Y, Sun L, Wang Q et al (2014) In-plane mesoporous graphene oxide nanosheet assembled membranes for molecular separation. RSC Adv 4:21425–21428
45. Hu M, Mi B (2013) Enabling graphene oxide nanosheets as water separation membranes. Environ Sci Technol 47:3715–3723
46. Sun P, Zhu M, Wang K et al (2013) Selective ion penetration of graphene oxide membranes. ACS Nano 7:428–437
47. Han Y, Xu Z, Gao C (2013) Ultrathin graphene nanofiltration membrane for water purification. Adv Funct Mater 23:3693–3700
48. Nair RR, Wu HA, Jayaram PN et al (2012) Unimpeded permeation of water through helium-leak–tight graphene-based membranes. Science 335:442–444
49. Mi B (2014) Graphene oxide membranes for ionic and molecular sieving. Science 343:740–742
50. Li H, Song Z, Zhang X et al (2013) Ultrathin, molecular-sieving graphene oxide membranes for selective hydrogen separation. Science 342:95–98
51. Joshi RK, Carbone P, Wang FC et al (2014) Precise and ultrafast molecular sieving through graphene oxide membranes. Science 343:752–754
52. Blankenburg S, Bieri M, Fasel R et al (2010) Porous graphene as an atmospheric nanofilter. Small 6:2266–2271
53. Du AJ, Zhu ZH, Smith SC (2010) Multifunctional porous graphene for nanoelectronics and hydrogen storage: new properties revealed by first principle calculations. J Am Chem Soc 132:2876–2877
54. Schrier J (2010) Helium separation using porous graphene membranes. J Phys Chem Lett 1:2284–2287
55. Xue Q, Shan M, Tao Y et al (2014) N-doped porous graphene for carbon dioxide separation: a molecular dynamics study. Chin Sci Bull 59:3919–3925
56. Celebi K, Buchheim J, Wyss RM et al (2014) Ultimate permeation across atomically thin porous graphene. Science 344:289–292
57. Cohen-Tanugi D, Grossman JC (2012) Water desalination across nanoporous graphene. Nano Lett 12:3602–3608
58. O'Hern SC, Boutilier MSH, Idrobo J-C et al (2014) Selective ionic transport through tunable subnanometer pores in single-layer graphene membranes. Nano Lett 14:1234–1241
59. Surwade SP, Smirnov SN, Vlassiouk IV et al (2015) Water desalination using nanoporous single-layer graphene. Nat Nanotechnol 10:459–464
60. Karnik RN (2014) Materials science: breakthrough for protons. Nature 516:173–175
61. Hauser AW, Schrier J, Schwerdtfeger P (2012) Helium tunneling through nitrogen-functionalized graphene pores: pressure- and temperature-driven approaches to isotope separation. J Phys Chem C 116:10819–10827
62. Hauser AW, Schwerdtfeger P (2011) Nanoporous graphene membranes for efficient $^3He/^4He$ separation. J Phys Chem Lett 3:209–213
63. Schrier J, McClain J (2012) Thermally-driven isotope separation across nanoporous graphene. Chem Phys Lett 521:118–124
64. Hankel M, Jiao Y, Du A et al (2012) Asymmetrically decorated, doped porous graphene as an effective membrane for hydrogen isotope separation. J Phys Chem C 116:6672–6676
65. Wang L, Drahushuk LW, Cantley L et al (2015) Molecular valves for controlling gas phase transport made from discrete ångström-sized pores in graphene. Nat Nanotechnol 10:785–790
66. Postma HWC (2010) Rapid sequencing of individual DNA molecules in graphene nanogaps. Nano Lett 10:420–425
67. Schneider GF, Kowalczyk SW, Calado VE et al (2010) DNA translocation through graphene nanopores. Nano Lett 10:3163–3167
68. Siwy ZS, Davenport M (2010) Nanopores: graphene opens up to DNA. Nat Nanotechnol 5:697–698
69. Schrier J (2012) Carbon dioxide separation with a two-dimensional polymer membrane. ACS Appl Mater Interface 4:3745–3752
70. Tao Y, Xue Q, Liu Z et al (2014) Tunable hydrogen separation in porous graphene membrane: first-principle and molecular dynamic simulation. ACS Appl Mater Interface 6:8048–8058
71. Wu T, Xue Q, Ling C et al (2014) Fluorine-modified porous graphene as membrane for CO_2/N_2 separation: molecular dynamic and first-principles simulations. J Phys Chem C 118:7369–7376
72. Liu H, Dai S, Jiang D (2013) Permeance of H_2 through porous graphene from molecular dynamics. Solid State Commun 175–176:101–105
73. Liu H, Dai S, Jiang D (2013) Insights into CO_2/N_2 separation through nanoporous graphene from molecular dynamics. Nanoscale 5:9984–9987
74. Liu H, Chen Z, Dai S et al (2015) Selectivity trend of gas separation through nanoporous graphene. J Solid State Chem 224:2–6

75. Sun C, Wen B, Bai B (2015) Application of nanoporous graphene membranes in natural gas processing: molecular simulations of CH_4/CO_2, CH_4/H_2S and CH_4/N_2 separation. Chem Eng Sci 138:616–621
76. Lu R, Rao D, Lu Z et al (2012) Prominently improved hydrogen purification and dispersive metal binding for hydrogen storage by substitutional doping in porous graphene. J Phys Chem C 116:21291–21296
77. Nieszporek K, Drach M (2015) Alkane separation using nanoporous graphene membranes. Phys Chem Chem Phys 17:1018–1024
78. Sun C, Boutilier MSH, Au H et al (2014) Mechanisms of molecular permeation through nanoporous graphene membranes. Langmuir 30:675–682
79. Ambrosetti A, Silvestrelli PL (2014) Gas separation in nanoporous graphene from first principle calculations. J Phys Chem C 118:19172–19179
80. Hauser AW, Schwerdtfeger P (2012) Methane-selective nanoporous graphene membranes for gas purification. Phys Chem Chem Phys 14:13292–13298
81. Qin X, Meng Q, Feng Y et al (2013) Graphene with line defect as a membrane for gas separation: design via a first-principles modeling. Surf Sci 607:153–158
82. Drahushuk LW, Strano MS (2012) Mechanisms of gas permeation through single layer graphene membranes. Langmuir 28:16671–16678
83. Shan M, Xue Q, Jing N et al (2012) Influence of chemical functionalization on the CO_2/N_2 separation performance of porous graphene membranes. Nanoscale 4:5477–5482
84. Lei G, Liu C, Xie H et al (2014) Separation of the hydrogen sulfide and methane mixture by the porous graphene membrane: effect of the charges. Chem Phys Lett 599:127–132
85. Huang C, Wu H, Deng K et al (2014) Improved permeability and selectivity in porous graphene for hydrogen purification. Phys Chem Chem Phys 16:25755–25759
86. Wen B, Sun C, Bai B (2015) Inhibition effect of a non-permeating component on gas permeability of nanoporous graphene membrane. Phys Chem Chem Phys 17:23619–23626
87. Boutilier MSH, Sun C, O'Hern SC et al (2014) Implications of permeation through intrinsic defects in graphene on the design of defect-tolerant membranes for gas separation. ACS Nano 8:841–849
88. Kim HW, Yoon HW, Yoon S-M et al (2013) Selective gas transport through few-layered graphene and graphene oxide membranes. Science 342:91–95
89. Konatham D, Yu J, Ho TA et al (2013) Simulation insights for graphene-based water desalination membranes. Langmuir 29: 11884–11897
90. Cohen-Tanugi D, McGovern RK, Dave SH et al (2014) Quantifying the potential of ultra-permeable membranes for water desalination. Energy Environ Sci 7:1134–1141
91. Zhu C, Li H, Zeng XC et al (2013) Quantized water transport: ideal desalination through graphyne-4 membrane. Sci Rep 3:3163
92. Zhu C, Li H, Meng S (2014) Transport behavior of water molecules through two-dimensional nanopores. J Chem Phys 141:18C528
93. Suk ME, Aluru NR (2010) Water transport through ultrathin graphene. J Phys Chem Lett 1:1590–1594
94. Cohen-Tanugi D, Grossman JC (2014) Water permeability of nanoporous graphene at realistic pressures for reverse osmosis desalination. J Chem Phys 141:074704
95. Cohen-Tanugi D, Grossman JC (2014) Mechanical strength of nanoporous graphene as a desalination membrane. Nano Lett 14:6171–6178
96. Hu G, Mao M, Ghosal S (2012) Ion transport through a graphene nanopore. Nanotechnology 23:395501
97. Suk ME, Aluru NR (2014) Ion transport in sub-5-nm graphene nanopores. J Chem Phys 140:084707
98. Zhao S, Xue J, Kang W (2013) Ion selection of charge-modified large nanopores in a graphene sheet. J Chem Phys 139:114702
99. O'Hern SC, Jang D, Bose S et al (2015) Nanofiltration across defect-sealed nanoporous monolayer graphene. Nano Lett 15:3254–3260
100. Azamat J, Khataee A, Joo SW (2015) Molecular dynamics simulation of trihalomethanes separation from water by functionalized nanoporous graphene under induced pressure. Chem Eng Sci 127:285–292
101. Kang Y, Zhang Z, Shi H et al (2014) Na^+ and K^+ ion selectivity by size-controlled biomimetic graphene nanopores. Nanoscale 6:10666–10672
102. Liang X, Fu Z, Chou SY (2007) Graphene transistors fabricated via transfer-printing in device active-areas on large wafer. Nano Lett 7:3840–3844
103. Liu L-H, Yan M (2009) Simple method for the covalent immobilization of graphene. Nano Lett 9:3375–3378
104. Reina A, Jia X, Ho J et al (2009) Large area, few-layer graphene films on arbitrary substrates by chemical vapor deposition. Nano Lett 9:30–35
105. Regan W, Alem N, Alemán B et al (2010) A direct transfer of layer-area graphene. Appl Phys Lett 96:113102
106. Caldwell JD, Anderson TJ, Culbertson JC et al (2010) Technique for the dry transfer of epitaxial graphene onto arbitrary substrates. ACS Nano 4:1108–1114
107. Allen MJ, Tung VC, Gomez L et al (2009) Soft transfer printing of chemically converted graphene. Adv Mater 21:2098–2102
108. Suk JW, Kitt A, Magnuson CW et al (2011) Transfer of CVD-grown monolayer graphene onto arbitrary substrates. ACS Nano 5:6916–6924
109. Fischbein MD, Drndić M (2008) Electron beam nanosculpting of suspended graphene sheets. Appl Phys Lett 93:113107
110. Safron NS, Brewer AS, Arnold MS (2011) Semiconducting two-dimensional graphene nanoconstriction arrays. Small 7:492–498
111. Fan Z, Zhao Q, Li T et al (2012) Easy synthesis of porous graphene nanosheets and their use in supercapacitors. Carbon 50:1699–1703
112. Fox D, O'Neill A, Zhou D et al (2011) Nitrogen assisted etching of graphene layers in a scanning electron microscope. Appl Phys Lett 98:243117
113. Liang X, Jung Y-S, Wu S et al (2010) Formation of bandgap and subbands in graphene nanomeshes with sub-10 nm ribbon width fabricated via nanoimprint lithography. Nano Lett 10: 2454–2460
114. Yuan W, Chen J, Shi G (2014) Nanoporous graphene materials. Mater Today 17:77–85
115. Safron NS, Kim M, Gopalan P et al (2012) Barrier-guided growth of micro- and nano-structured graphene. Adv Mater 24:1041–1045
116. Ning G, Fan Z, Wang G et al (2011) Gram-scale synthesis of nanomesh graphene with high surface area and its application in supercapacitor electrodes. Chem Commun 47:5976–5978
117. Wang M, Fu L, Gan L et al (2013) CVD growth of large area smooth-edged graphene nanomesh by nanosphere lithography. Sci Rep 3:1238
118. Paul RK, Badhulika S, Saucedo NM et al (2012) Graphene nanomesh as highly sensitive chemiresistor gas sensor. Anal Chem 84:8171–8178
119. Koh D-Y, Lively RP (2015) Nanoporous graphene: membranes at the limit. Nat Nanotechnol 10:385–386